Novel Small-Molecule Inhibitors of Anthrax Lethal Factor Identified by High-Throughput Screening

Igor A. Schepetkin,[†] Andrei I. Khlebnikov,[‡] Liliya N. Kirpotina,[†] and Mark T. Quinn*,[†]

Department of Veterinary Molecular Biology, Montana State University, Bozeman, Montana 59717, and Department of Chemistry, Altai State Technical University, Barnaul 656038, Russia

Anthrax lethal factor (LF) is a key virulence factor of anthrax lethal toxin. We screened a chemolibrary of 10 000 drug-like molecules for their ability to inhibit LF and identified 18 novel small molecules with potent LF inhibitory activity. Three additional LF inhibitors were identified through further structure−activity relationship (SAR) analysis. All 21 compounds inhibited LF with an IC_{50} range of 0.8 to 11 μM, utilizing mixed-mode competitive inhibition. An evaluation of inhibitory activity against a range of unrelated proteases showed relatively high specificity for LF. Furthermore, pharmacophore modeling of these compounds showed a high degree of similarity to the model published by Panchal et al. (*Nat. Struct. Mol. Biol.* **2004**, *11*, 67−72), indicating that the conformational features of these inhibitors are structurally compatible with the steric constraints of the substrate-binding pocket. These novel LF inhibitors and the structural scaffolds identified as important for inhibitory activity represent promising leads to pursue for further LF inhibitor development.

Introduction

Anthrax is an acute infectious disease caused by toxigenic strains of the spore-forming bacterium *Bacillus anthracis*. This disease occurs most commonly in agricultural regions, where it can be found in livestock and wild animals. Naturally occurring anthrax is extremely rare in humans and is primarily associated with exposure to infected animals or tissue from infected animals.[1] However, recent events have demonstrated that *B. anthracis* now poses a significant threat as an agent of biological warfare and terrorism, with a significant capacity to cause mortality.[2]

The major virulence factor of *B. anthracis* is anthrax toxin, which is a binary A−B toxin comprised of protective antigen (PA[a], 87.2 kDa)[1] and two enzymatic moieties, lethal factor (LF, 90.2 kDa) and edema factor (EF, 88.8 kDa).[3,4] PA binds to cell-surface receptors and is cleaved by furin-like proteases to form 63 kDa fragments (PA63) that oligomerize into homoheptameric pores and bind LF and EF.[5] Oligomerization also triggers endocytosis of the receptor-bound PA63−LF−EF complex by a clathrin-mediated process. Subsequently, LF and EF are packaged into endosomal carrier vesicles and delivered to the cytoplasm by release from late endosomes.[5]

LF appears to be critical for pathogenesis, and bacterial strains lacking LF are not lethal in mice.[6] LF is a Zn^{2+}-dependent endopeptidase, which specifically cleaves mitogen-activated protein kinase kinases (MAPKK) near their *N*-termini, thereby interfering with MAPK-dependent signaling pathways that recruit other immune cells during the response to inflammatory stress.[4] Although antibiotics are effective in clearing *B. anthracis* from the organism, high levels of the toxin may remain in circulation for several days. Thus, combination therapies of antibiotics and toxin inhibitors have been proposed.[7]

There are many potential targets for therapeutic intervention against anthrax lethal toxin (i.e., complex of PA and LF), and new strategies have been exploited on the basis of the recent understanding of the structure and function of the toxin proteins. These approaches include inhibitors of furin-related proteases to block the proteolytic activation of PA,[8] recombinant antibodies against PA,[9] and polyvalent inhibitors of PA−LF interactions.[10] Because of the key role played by LF in pathogenesis, a number of studies have also focused on the development of LF inhibitors. For example, the lethal action of anthrax toxin can be blocked by synthetic or natural substances that inhibit LF protease activity.[11−13] Peptide and small-molecule LF inhibitors have also been pursued as potential sources of new therapeutics to treat anthrax,[14−24] although relatively few potent competitive and noncompetitive LF inhibitors have been found.

Many LF inhibitors have been identified by high-throughput screening (HTS) of libraries composed of a variety of synthetic and natural compounds.[14,17−19,21,22,25] Of note, Panchal et al.[14] used HTS to screen a 1900-compound chemolibrary for LF inhibitors and identified 19 compounds with IC_{50} <20 μM. Using structures of six selected compounds that showed a range of LF inhibitory potency, the authors established a six-point pharmacophore model of LF inhibitors.[14] This model suggested several common features essential for optimal LF inhibitor binding and provides a rational approach for optimization of candidate small-molecule inhibitors.

In the present study, we utilized HTS to screen a chemical diversity library containing 10 000 drug-like molecules to identify novel inhibitors of LF that have core structures distinct from currently known leads. We identified 21 small molecules that were potent inhibitors of LF protease activity (IC_{50} values of 0.5−11 μM), many highly selective for LF. In addition, we used substructure screening, fragment-focusing, and structure−activity relationship (SAR) analyses to further probe the parent chemical library and defined at least three groups of LF inhibitors: carboxylic acid derivatives of 2-phenylfurans, *N*-phenyldihydropyrazoles, and *N*-phenylpyrroles. A compound-based pharmacophore modeling of these inhibitors showed a

---

* To whom correspondence should be addressed. Phone: 406-994-5721. Fax: 406-994-4303. E-mail: mquinn@montana.edu.
† Montana State University.
‡ Altai State Technical University.
[a] Abbreviations: PA, protective antigen; LF, lethal factor; EF, edema factor; HTS, high-throughput screening; SAR, structure−activity relationship; MMP, matrix metalloproteinase.
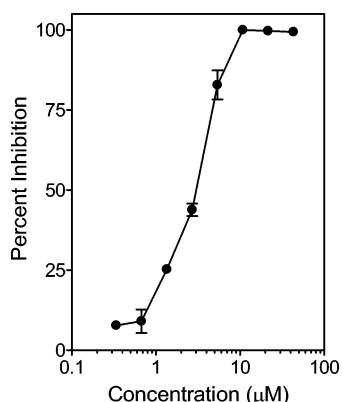
Figure 1. Inhibition of LF protease activity by a representative compound identified with high-throughput screening. Recombinant LF was incubated with the indicated concentrations of compound **10**, and cleavage of fluorogenic LF protease substrate was monitored, as described. The percent inhibition of LF activity is plotted against logarithm of inhibitor concentration. Data are presented as the mean ± SD of four replicates. A representative experiment from three independent experiments is shown.

strong correlation to the current pharmacophore model of LF inhibitors, which was based on the X-ray crystal structure of a small-molecule inhibitor bound to LF.[14]

Results and Discussion

Primary High-Throughput Screening. To identify novel compounds that inhibit LF protease activity, we screened a chemical diversity library of 10 000 drug-like compounds. This library was randomly assembled to maximize chemical diversity with commonly accepted pharmaceutical hit structures, including 810 nonfunctionalized carboxylic acid derivatives. However, it did not contain compounds with hydroxamate groups or with aminoglycoside, tetracycline, and gallate scaffolds, all which have been reported previously as LF inhibitors.[15,17−20,25]

A compound was defined as a hit if it exhibited >75% inhibition of LF activity, with a final compound concentration of 20 μg/mL in fluorescence-based microplate assays. From the primary enzymatic screening, 391 inhibitory compounds were selected (3.9% hit rate). The size of the hit set was further reduced by applying a series of experimental filters to eliminate crystallite- and aggregate-forming compounds, which could nonspecifically inhibit enzymatic activity by absorption of enzyme molecules to/into the aggregates.[26] These filters included determination of the solubility of selected compounds, evaluation of nonspecific LF inhibitory activity in the presence of 0.01% (w/v) bovine serum albumin, and measuring the dose−response relationship for enzyme inhibition.[26,27] The dose−response relationship of 49 compounds resulted in typical sigmoidal semilogarithmic curves associated with desirable inhibitors. As an example, a representative curve for compound **10** is shown in Figure 1. Eighteen compounds with the highest inhibitory activity for LF (IC$_{50}$ <11 μM) were selected as a set of prospective LF inhibitors, and the structures of these compounds and their activities are presented in Figure 2 and Table 1, respectively.

To eliminate false positives resulting from fluorescence quenching by test compounds, high-performance liquid chromatography (HPLC) was used to separate the cleavage product and inhibitor compounds.[14] The separated cleavage product was then quantified in the absence of inhibitor, allowing us to evaluate fluorescence quenching by the compounds (example shown in Figure 3). For most of the compounds (13 of 18),

IC$_{50}$ values obtained by the microplate and HPLC assays were quite close, falling <15% of each other and indicating that the observed inhibition was not due to nonspecific quenching of the fluorescence signal (Table 1). In contrast, the apparent IC$_{50}$ values of compounds **1**, **9**, **13**, **15**, and **17** obtained by the microplate assay were 15−35% lower than those from the HPLC-based assay, suggesting the possible quenching of part of the product fluorescence by these compounds.

Kinetic Features of Selected Inhibitors. For the selected compounds, LF inhibition occurred rapidly after the addition of inhibitor, with no lag period. As an example, reaction kinetics measured at different concentrations of compound **10** are shown in Figure 4A and indicate that the compound is a rapid inhibitor of LF protease activity. Dixon plots for hydrolysis of the fluorogenic substrate (2.5−20 μM) by LF (5 nM) in the absence and in the presence of the compounds (0.625−10 μg/mL) showed linear mixed-type inhibition for all 18 compounds (Table 1), suggesting that these compounds can bind directly to LF as well as to the LF−substrate complex. Double-reciprocal Lineweaver−Burk plots intersected at a single point above the abscissa (data for compound **17** are shown as an example in Figure 4B), confirming mixed or partial competitive inhibition and indicated that the inhibition constant K_i for binding to the free enzyme was greater than K_i' for binding to the LF−substrate complex (α > 1, where $K_i' = \alpha K_i$).[28] For most compounds, affinity to LF was in the range of 0.8−3.5 μM. The mixed-type inhibition observed for all of the selected inhibitors is likely due to the architecture of the LF substrate-binding region, which appears to be an extended 40 Å groove.[15,29] This conformation may allow inhibitors to bind to the LF adjacent to the cleavage site and interfere at varying degrees with substrate binding. Thus, occlusion of a portion of the catalytic pocket by such an LF inhibitor could prevent substrate access to the catalytic residues, or the peptide substrate could bind in a nonproductive mode. Another possibility is that some of these inhibitors may bind to both the peptide- and water-binding sites[30] and could be classified as multisubstrate inhibitors.[31]

Specificity of Selected Inhibitors. To evaluate inhibitor specificity, we analyzed the effects of the selected compounds on six different proteases unrelated to the LF. These proteases included two Zn^{2+}-dependent proteases (porcine kidney aminopeptidase M (EC 3.4.11.2) and human matrix metalloproteinase-9 (MMP-9) (EC 3.4.24.35)), three serine proteases (human pancreatic chymotrypsin (EC 3.4.21.1), human plasma kallikrein (EC 3.4.21.34), and human neutrophil elastase (EC 3.4.21.37)), and a cysteine protease (human liver cathepsin B (EC 3.4.22.1)). As shown in Table 1, many of the selected compounds were quite specific for LF. None of the selected compounds inhibited aminopeptidase M, and most of the compounds also did not inhibit chymotrypsin or MMP-9. Seven of the compounds (**2**, **7**, **9**, **11−13**, and **16**) were highly specific, either inhibiting none or only weakly inhibiting one of the other proteases tested. These data further confirmed that LF inhibition was not due to nonspecific effects of the test compounds. The activity of kallikrein was inhibited by compounds **1**, **7**, **8**, **10**, **11**, and **15** at relatively low concentrations (IC$_{50}$ values of 5−36 μM). Among these compounds, the nitrile **15** was a relatively potent kallikrein inhibitor, with IC$_{50}$ = 5.5 μM. It should be noted that several nitrile derivatives have been found previously to be inhibitors of serine proteases.[32] Overall, this preliminary characterization of specificity indicates that a number of the selected LF inhibitors are relatively selective for LF and may be the most promising leads for further characterization and optimization.
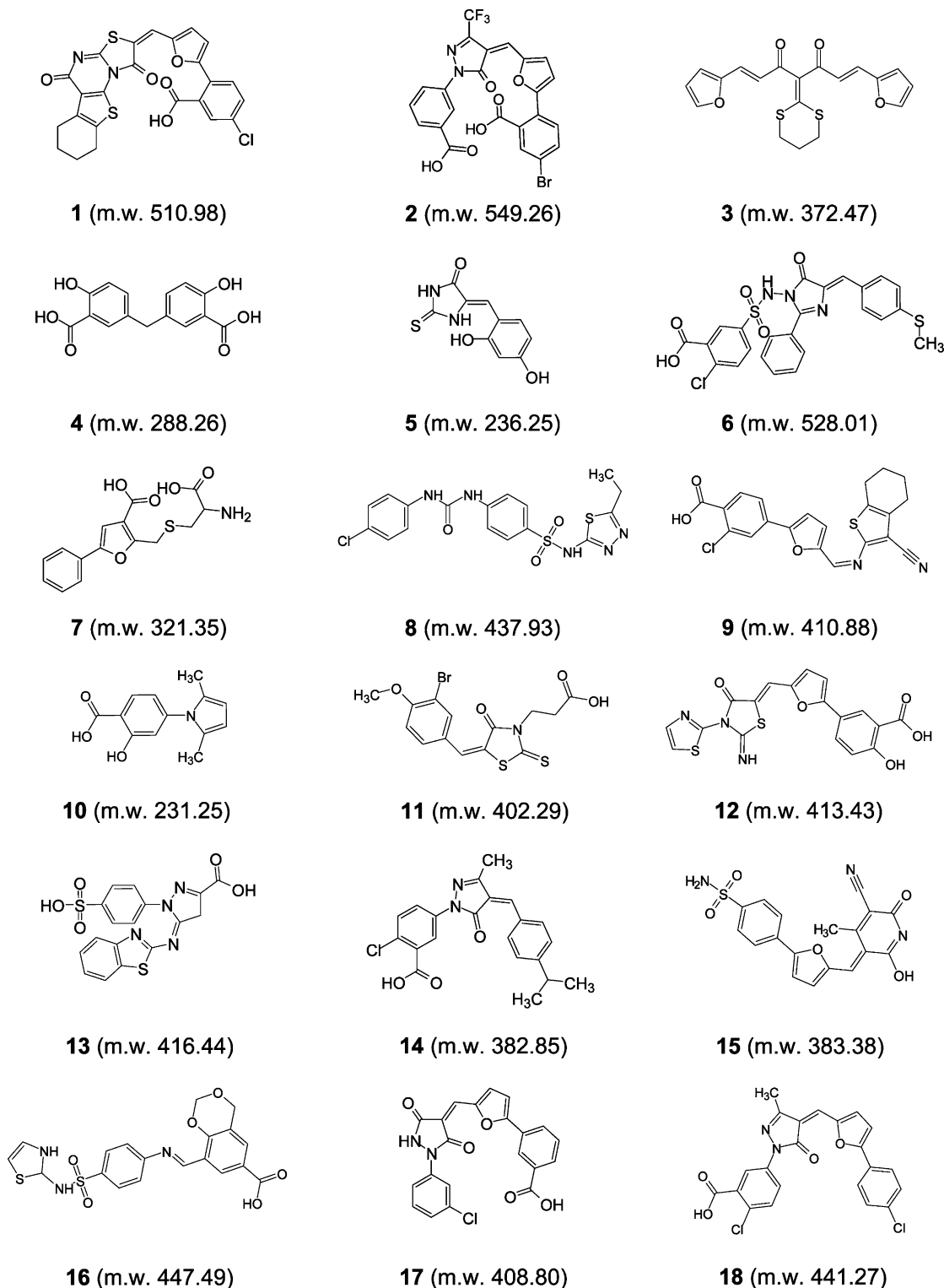
Figure 2. Chemical structures and molecular weights of the most potent LF inhibitors identified with high-throughput screening. Compounds with IC$_{50}$ values <11 μM are shown. The compound numbers indicated in bold are used in this article to designate each compound.

Substructure Analysis and Fragment Focusing. Several molecular substructures and scaffolds essential for the activity of synthetic nonhydroxamate LF inhibitors have been reported.[14,16−22,25] Although some of these substructures were included in the parent chemical diversity library, most compounds with the indicated fragments and scaffolds, with the exception of compound **8**, were not present in the highly active prospective set because their IC$_{50}$ values were >11 μM (Table 2). One reason for the lower activities of these compounds may be that they lacked the additional constituents necessary to convey a high level of inhibitory activity. It should be noted that the compound shown in row 2, column 5 of Table 2 (IC$_{50}$ = 28.3 μM) was previously identified as a low-activity LF inhibitor with IC$_{50}$ = 140 μM.[22] The difference in potency observed here may be due to the differences in the methods used to monitor LF cleavage kinetics or the possible differences in compound quality.

An examination of the 18 structures representing the most potent LF inhibitors (Table 1) resulted in the grouping of most compounds with two main classes of molecular fragments:

Table 1. Kinetic Characteristics of the Eighteen Most Potent LF Inhibitors Identified by High-Throughput Screening and Evaluation of Specificity

	lethal factor					other proteases IC_{50} (μM)						highest tested concn (μM)
compd no.	IC_{50} (μM) microplate assay	IC_{50} (μM) HPLC assay	K_i (μM)	K_i' (μM)	mode of inhibition	aminopeptidase M	chymotrypsin	kallikrein	elastase	cathepsin B	MMP-9	
1	0.8	1.1	0.8	2.6	mixed	N.I.[a]	72.6	13.5	19.6	59.4	N.I.	80
2	1.7	1.8	1.6	2.4	mixed	N.I.	N.I.	N.I.	N.I.	32.1	N.I.	75
3	3.0	3.2	2.7	4.9	mixed	N.I.	90.3	67.4	6.7	26.9	N.I.	135
4	3.1	2.9	2.4	4.9	mixed	N.I.	N.I.	67.9	N.I.	90.2	43.4	175
5	3.4	3.7	1.1	15.2	mixed	N.I.	143.6	120.1	84.8	52.3	105.9	220
6	3.6	3.3	2.5	4.7	mixed	N.I.	N.I.	N.I.	75.8	63.1	29.6	100
7	3.6	4.1	2.9	4.1	mixed	N.I.	N.I.	35.4	N.I.	N.I.	N.I.	125
8	3.9	4.8	0.9	11.5	mixed	N.I.	N.I.	28.1	78.3	5.2	N.I.	115
9	4.2	5.2	2.4	5.6	mixed	N.I.	N.I.	46.2	N.I.	N.I.	N.I.	100
10	4.3	3.8	1.5	6.7	mixed	N.I.	N.I.	30.1	51.5	55.0	43.0	220
11	4.4	4.7	3.3	5.2	mixed	N.I.	N.I.	31.7	N.I.	N.I.	N.I.	100
12	4.8	4.2	3.1	5.6	mixed	N.I.	N.I.	N.I.	N.I.	72.3	N.I.	120
13	7.7	9.2	4.2	9.7	mixed	N.I.	N.I.	N.I.	N.I.	N.I.	60.1	120
14	7.9	8.2	0.9	13.1	mixed	N.I.	N.I.	54.2	N.I.	22.4	N.I.	100
15	8.3	10.8	5.4	15.2	mixed	N.I.	74.1	5.5	52.2	64.8	N.I.	100
16	9.3	8.7	1.8	20.9	mixed	N.I.	N.I.	N.I.	N.I.	N.I.	N.I.	90
17	10.5	13.9	7.2	15.1	mixed	N.I.	N.I.	96.2	N.I.	81.5	N.I.	125
18	10.7	10.0	2.1	19.5	mixed	N.I.	N.I.	75.0	89.8	88.9	N.I.	90

[a] N.I., no inhibition seen at the highest concentration of compound tested (see the last column of the Table).
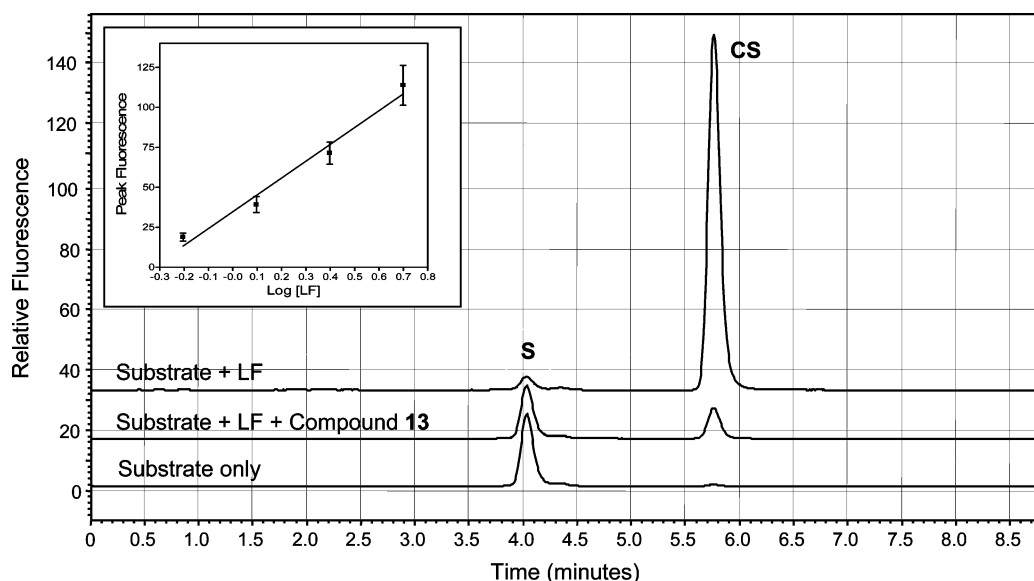

Figure 3. Analysis of LF inhibitors by HPLC. A representative HPLC profile is shown for determining the inhibitory activity of selected compounds. LF was incubated for 30 min with compound **13** or a vehicle, and the incubation was terminated by the addition 9 volumes of 70% acetonitrile in water (v/v) containing 0.1% TFA. Reaction samples were separated by HPLC, and fluorescent peaks representing the parent fluorogenic substrate (S) and *C*-terminal cleavage product (CS) were monitored, as described. For comparison, a control run using only the intact substrate (S) is also shown. Inset: Rate of change in peak fluorescence of CS vs the logarithm of concentration of LF (nM).

2-phenylfurans (compounds **1**, **7**, **9**, **12**, **15**, and **17**) and *N*-phenyldihydropyrazoles (compounds **13** and **14**). Compounds **2** and **18** possess both fragments. In addition, the set of active LF inhibitors also contained phenylimidazole, phenylpyrrole, and phenylpyrazolidine substructures (compounds **6**, **10**, and **17**, respectively), which were isosteric to phenylfuran and phenyldihydropyrazole moieties. In these fragments, the benzene ring was linked directly to one of the heterocycles (designated as substructure I), and 12 of the 18 active compounds contained substructure I (Table 3). Thus, this substructure seems to contribute to the interaction of these inhibitors with LF. It should be noted that substructures I, II, V, VI, VIII, IX, and X have all been previously reported to be present in various LF inhibitors.[21,22]

Methylidene and imino moieties may be optimal linkers because 10 of the 18 high-activity LF inhibitors contained these

linkers in compounds with substructures III−VI and VIII−X (Table 3). Consistent with this finding, the methylidene linker was present in all LF inhibitors reported previously by Forino and co-workers.[21,22] The presence of a double bond in the methylidene moiety suggests the possibility of *cis−trans* isomerism in some inhibitor molecules, and we found that the active compounds only had a *cis* configuration. In these inhibitors, an external substituent at the exocyclic double bond was oriented in the *cis* position to a neighboring electron-withdrawing group in the cycle, that is, a nitrogen in inhibitors **5** and **6** and a carbonyl group in inhibitors **1**, **2**, **11**, **14**, **17**, and **18** (Figure 2). It appears that an unsubstituted carboxyl group may be important for activity because ~78% of the active compounds were nonfunctionalized carboxylic acids (Table 1). Indeed, the presence of a free carboxylic acid group increased the activity of a variety of compounds by ~4−9-fold (Table 3;
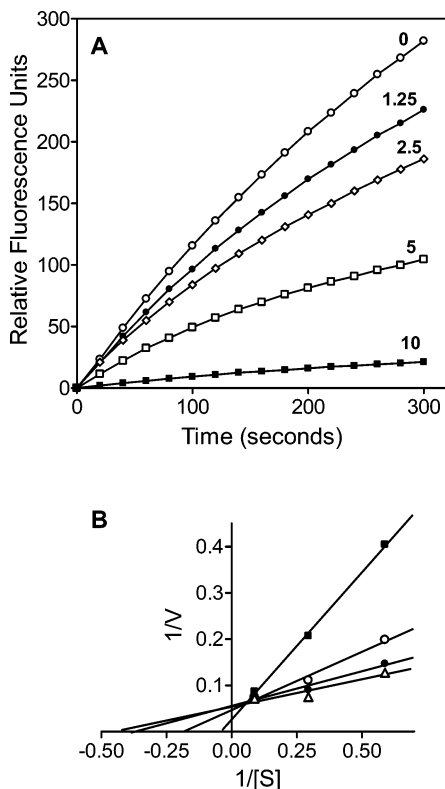
Figure 4. Kinetics of inhibition of LF protease activity by a representative compound identified with high-throughput screening. Panel A: Kinetic curves of fluorogenic substrate cleavage catalyzed by LF at different concentrations of compound **10**. Panel B: Double-reciprocal Lineweaver−Burk plot of LF inhibition by compound **17**. The concentrations of compound **17** were 0 (■), 3 (○), 6 (●), and 12 μM (△), and LF concentration was 5 nM. A representative experiment from three independent experiments is shown.

compare activities of compounds containing substructures I, III, V, and IX with those of compounds containing substructures II, IV, VI, and X, respectively, which also contain a free carboxyl group). Carboxyl groups possess potent Zn^{2+}-binding activity, although less than that of hydroxamate and thiol groups,[33] and this may contribute to the observed activity.

Fragment-based focusing was used to probe the parent chemical diversity library for substructures enriched in the selected LF inhibitors (Table 4). In the set of active compounds ($n = 18$), p-sulfonamido-N,N'-diphenylurea, carboxyphenol, 2-(carboxyphenyl)furan, N-(carboxyphenyl)-4,5-dihydropyrazole, and N-(carboxyphenyl)pyrrole substructures were enriched >100-fold compared to the parent set ($n = 10\,000$). Consistent with this observation, phenylfuran, phenypyrazole, and phenylpyrrole substructures are among the most common pharmacophoric moieties present in inhibitors of LF and other proteases.[21,22,34−37] Furthermore, previous molecular modeling studies indicate that pyrrole is a submolecule that improves the activity of LF inhibitors.[14] Thus, three series of carboxylic acid derivatives containing 2-phenylfuran, N-phenyldihydropyrazole, and N-phenylpyrrole substructures were extracted from the parent chemical diversity set for further structure−activity relationship (SAR) analyses, as described below. N-sulfonylated 2-phenylfuran and N-phenyldihydropyrazole derivatives were also considered because of their water solubility. Carboxy functionalized ester and/or lactone derivatives of these substructures were not considered, however, because of the apparent contribution of a free carboxyl group to LF inhibitory activity. Indeed, ester and lactone derivatives of phenylfurans, phe-

nyldihydropyrazoles, and phenylpyrroles (23 compounds) were inactive or only had low activity in the enzymatic assay (data not shown). Note that the small subset size of the p-sulfonamido-N,N'-diphenylureas (6 water-soluble compounds) did not allow us to perform SAR analysis of these inhibitors in the present studies.

Carboxylic and Sulfonamide 2-Phenylfuran Derivatives. The parent chemical diversity library contained 26 water-soluble carboxylic 2-phenylfuran derivatives. Seven of these compounds were active LF inhibitors (IC_{50} <11 μM; hit rate of 39%) with the best compounds **1** and **2** having an IC_{50} of <2 μM, whereas 12 other compounds had moderate to low activity (IC_{50} values of 14−50 μM) in the microplate-based enzymatic assay (Supporting Information, Table S1).
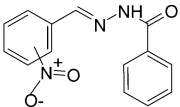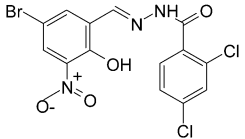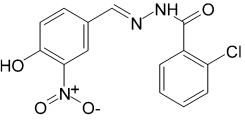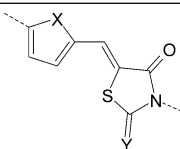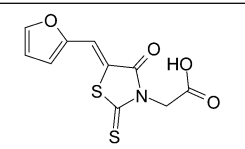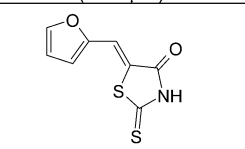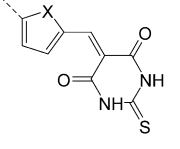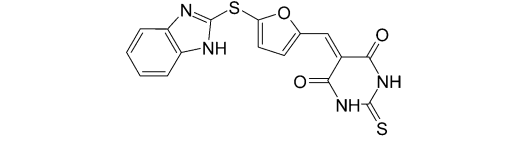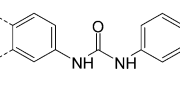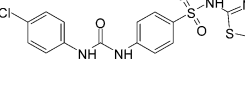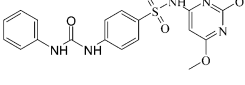
On the basis of a detailed analysis of substituents in the series of phenylfurans and consideration of LF inhibitory activity, we conclude that the highly active LF inhibitors (compounds **1**, **2**, **9**, **12**, **17**, and **18**) possessed considerably more rigid R^1 groups with fused heterocyclic systems or two rings separated by one chemical bond. These data suggest that optimal distances between key centers interacting with the enzyme site may be determined by this rigidity. The only exception to this paradigm was compound **7**, which also has a low molecular weight and, thus, may differ from the other inhibitors in its coordination with the enzyme.

Among the carboxylic derivatives, low-activity phenylfurans **21**, **22**, **25**−**27**, and **30** and nonactive compounds **32**, **34**, and **36** had only one ring (benzene or heterocycle) present as substituent R^1. Even if R^1 contained two rings separated by one bond (compounds **24** and **31**) or fused rings (compound **33**), the cycle in R^1 group was linked with the furan moiety by a chain longer than two chemical bonds. Thus, the optimal linker between the cycle in R^1 and furan moiety seems to be a methylidene group, and our data suggest that this linker may ensure that the required distances and suitable degree of rigidity are maintained in the whole R^1 substructure. Indeed, this linker is present in all of the active phenylfuran compounds, except for inhibitor **9**, which possesses a very similar imino linker. In some cases low-activity and nonactive carboxylic phenylfuran derivatives also contained an optimal methylidene linker; however, these compounds lacked other important features. As mentioned above, the presence of a free carboxyl group was necessary for optimal inhibitory activity, and the preferred location of this substituent was in the phenylfuran moiety, rather than in the phenyl ring of the R^1 group.

The inhibitory activity of N-sulfonylated phenylfuran derivatives was also evaluated because the presence of this substituent strongly enhances compound solubility. However, the sulfonamide group has low nucleophilicity and does not form stable complexes with metal ions.[38] The parent chemical diversity library contained 9 N-sulfonamide 2-phenylfuran derivatives (compounds **15**, **38**−**45**). In contrast to the carboxylic acid derivatives, the sulfonamide derivatives were not efficient LF inhibitors. Even though six of these compounds (**15**, **38**, **40**, **41**, **43**, and **44**) had the desirable substructures mentioned above, only compound **15** had high activity. Thus, these data further support the importance of a free carboxyl group in enzyme inhibition.

Carboxylic and Sulfonamide Derivatives of 1-Phenyl-4,5-dihydro-5-pyrazolone. The parent chemical diversity library contained 10 carboxylic and 5 sulfonamide water-soluble derivatives of 1-phenyl-4,5-dihydro-5-pyrazolone (see Supporting Information, Table S2). All high-activity compounds (IC_{50} <11 μM) had a carboxyl group in position R^4 of the benzene

Table 2. Substructures Present in Previously Reported LF Inhibitors and Their Distributions in the Parent Compound Library[a]

Substructures in Previously Reported LF Inhibitors	References	Number of Compounds w/ Substructure in Parent Library	Hit Rate (%)[b]	Structure of Active Compounds in Parent Library w/ Indicated Substructure (IC$_{50}$)	
	16	19	6.7	(35.5 μM)	(56.9 μM)
X= O or S; Y= O or S	21, 22	(X=O,Y=S), 9; (X=O,Y=O), 1; (X=S, Y=S), 5	13.3	(28.3 μM)	(56.4 μM)
X= O or S	22	(X=O), 6; (X=S), 2	12.5	(30.9 μM)	
	14	69	2.9	Compound **8** (3.9 μM)	(15.3 μM)

[a] The randomly selected 10 000-compound parent library did not contain several compounds/structures found previoiusly in LF inhibitors, including hydroxamates, aminoglycosides, catechin-gallates, and gallate-like polyphenols.[17–19,25] [b] For determining hit rate, compounds were considered active if IC$_{50}$ <60 μM in enzymatic assays.

ring and the optimal methylidene linker between the pyrazole moiety and furan cycle (inhibitors **2** and **18**) or pyrazole moiety and benzene ring (inhibitor **14**). Nonactive and low-activity compounds had no aromatic/heterocycle fragments in R^2 (compounds **46** and **51**), or the linker between the pyrazole moiety and benzene ring in R^2 consisted of more than two bonds (compounds **47** and **50**). Although the low-activity and nonactive derivatives **45** and **48−49** also contained a methylidene linker, they contained only one cycle fragment in R^2 (compounds **45** and **48**) and/or the carboxyl group was in the unfavorable R^5 position (compounds **49** and **50**).
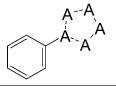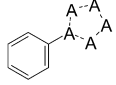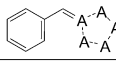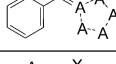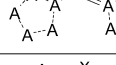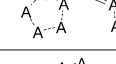
All sulfonamide derivatives had low activity (**52** and **53**) or were not active (**38**, **54**, and **55**). It should be noted that inactive sulfonamide compounds **38** and **52** had a preferred phenylfuran-methylidene-phenylpyrazole substructure; however, they lacked the necessary carboxyl group, which may form coordination bonds with the catalytic Zn^{2+}.
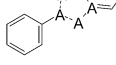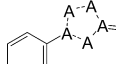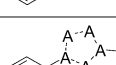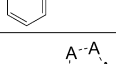
Carboxylic *N*-Phenylpyrrole Derivatives. The parent chemical diversity library contained 10 water-soluble carboxylic *N*-phenylpyrrole derivatives. To increase the number of compounds in this set, seven analogues with various substituents in the ortho, meta, or para positions of the phenyl ring were obtained commercially so that 17 carboxylic *N*-phenylpyrrole derivatives were included in the SAR study (see Supporting Information, Table S3). On the basis of kinetic assays, the most potent compounds (**10**, **56−58**) were mixed-mode inhibitors (Tables 1 and 5). In addition, compounds **56−58** were relatively selective for LF compared to the that of the six unrelated proteases tested (Table 5). Thus, these compounds also represent reasonable leads for further optimization and evaluation of specificity.

The small subset size of carboxylic phenylpyrrole derivatives (see Supporting Information, Table S3) did not allow us to perform a systematic SAR analysis of these inhibitors. However, some details of their chemical structures made it possible to define differences between active and inactive pyrroles. For example, the substitution of the hydroxyl group in compound **10** with a chlorine atom (compound **71**) significantly reduced LF inhibitory activity. Perhaps a hydroxyl group in this position plays a role in the enzyme−inhibitor interaction of pyrrole **10**, forming a hydrogen bond with an appropriate counterpart in the active site. This idea is supported by the fact that compound **68**, which lacks an analogous hydroxyl group, was inactive. In addition, switching the carboxyl and hydroxyl substituents in compound **10** (see compound **69**) resulted in a loss of activity. Interestingly, relocation of the carboxyl group from the para position in pyrrole **68** to the meta position (compound **59**) enhanced activity. However, moving the carboxyl group to the ortho position (compound **70**) resulted in a complete loss of activity. Certain placements of chlorine atoms may also contribute to ligand recognition because chlorinated benzene derivatives possessed higher polarity and polarizability, and this may promote binding with polar centers in the enzyme. For example, compound **57** was twice as active as its nonchlorinated analogue (compound **59**).

The exchange of hydrogen in the R^2 position of compound **59** with a bulky substituent (see compounds **60** and **64**) led to a loss of LF inhibitory activity. Nonactive compounds **61** and **65−67** lacked a free carboxyl group in the benzene ring. Additionally, these compounds also had large substituents instead of a methyl group in the R^1 and R^3 positions. The *N*-phenylpyrrole is a planar and rigid electron donor−acceptor

Table 3. Basic Substructures of the Selected LF Inhibitors and Their Distribution in the Parent Compound Library

	Substructure[a]	Total % of Compounds w/ Substructure in Parent Library	% of Active Compounds w/ Substructure	
			in Active Set[b]	in Parent Library
I	(phenyl with five-membered ring)	12.37	66.7	1.0
II	(phenyl with five-membered ring) and COOH	1.46	61.1	7.5
III	(benzene linked to five-membered ring)	1.68	22.2	2.4
IV	(benzene linked to five-membered ring) and COOH	0.14	16.7	21.4
V	(two five-membered rings, X= CH or N)	0.83	33.3	7.2
VI	(two five-membered rings) and COOH (X= CH or N)	0.09	33.3	66.7
VII	(phenyl, five-membered ring) *trans* conformation	0.49	0	0
VIII	(phenyl, five-membered ring) *cis* conformation	0.63	27.8	7.9
IX	(phenyl, five-membered ring)	0.63	27.8	7.9
X	(phenyl, five-membered ring) and COOH	0.17	27.8	29.4

[a] Dashed lines represent any bond type, and A represents any atom except hydrogen. [b] The number of compounds in the active set was 18 (see Table 1 and Figure 2).
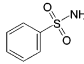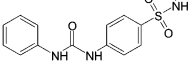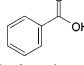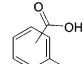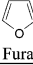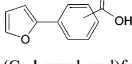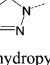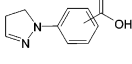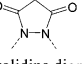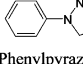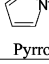
substructure with fast intramolecular charge transfer.[39] However, the inclusion of more bulky α-substituents in the pyrrole ring may force the *N*-phenyl group out of the plane of the heterocycle[40] or introduce steric interference, resulting in less favorable interactions with the enzyme. In support of this idea, inactive compound **62** contains a large side chain in the pyrrole ring at position R[2], whereas active compound **59** lacks this substituent. Similarly, the incorporation of a CH₂ between the benzene ring and carboxyl group in compound **68** converts this nonactive compound into a compound with inhibitory activity (compound **58**). Furthermore, lengthening the chain by a sulfur bridge enhanced inhibitory activity even more (see compound **56**). However, this effect may also be due to the presence of vacant *d*-orbitals and other specific properties of the sulfur atom, rather than the bulk of the substituent.

Conformational Analysis and Pharmacophore Modeling. Recently, Panchal et al.[14] developed a six-point pharmacophore model of LF inhibitors that was based on overlapping conformations of LF inhibitors and a comparison with the X-ray crystal structure of one of these inhibitors bound to LF. This model is characterized by axial symmetry of hydrophobic (aromatic) centers **A** and **B** separated by a polar center **D** and a linker **F** Figure 5A). Two other peripheral polar centers, **C** and **E**, are located in the vicinity of the hydrophobic groups. The hydrophobic center in inhibitory molecules seems to be essential for binding because the catalytic site of LF contains a hydrophobic substrate-binding groove.[14,15] In the present studies, we evaluated this model using an independent set of LF inhibitors.

From screening data, we identified 21 compounds with potent LF inhibitory activity (Tables 1 and 5). Although these inhibitors represent a diverse set of compounds, a visua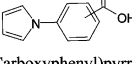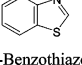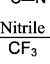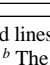l inspection of their structures allowed us to identify a phenyl-substituted five-membered ring comprising a polar group (carbonyl or furan oxygen) in many of the selected compounds. Moreover, the benzene ring in this substructure also contained polar substituents, which correlated well with centers **B**, **D** and **E** of the pharmacophore model.[14] Taking into account that most of the five-membered rings are connected with other bulky groups of aromatic and heteroaromatic nature associated with center **A**, one can see the obvious similarity of these structures to that of the pharmacophore model.

To identify the pharmacophoric centers in our active LF inhibitors, we performed conformational analysis of 11 highly active compounds from Table 1 (**1**, **2**, **5**, **7**−**10**, **12**, **15**, **17**, and **18**). Considering that these are flexible molecules, we explored their potential energy surfaces using a conformational search with an MM+ force field. The conformations within an energy gap of 6 kcal/mol over the global minimum[41] were stored and subjected to cluster analysis[42] to identify the representative conformers, and the number of clusters obtained for the LF inhibitors are presented in Table 6. Optimization of the lowest-energy conformation from each cluster by the PM3 method led to a set of geometric structures for further overlay and analysis of pharmacophoric features. The number of representative conformations differed significantly, depending on the flexibility of the compounds. As shown in Table 6, the most active

Table 4. Functional Groups Present in the Selected LF Inhibitors and Their Distribution in the Parent Compound Library

Substructure[a]	% of Compounds w/ Substructure in Parent Library	% of Active Compounds w/ Substructure	
		in Active Set[b]	in Parent Library
Benzene-sulfonamide	7.23	22.2	0.6
N,N'-diphenylurea-sulfonamide	0.07	5.6	14.3
Carboxybenzene	2.92	55.6	3.4
Carboxyphenol	0.17	16.7	17.6
Furan	7.3	44.4	1.1
2-(Carboxyphenyl)furan	0.28	27.8	17.9
4,5-Dihydropyrazole	0.72	22.2	5.6
N-Carboxyphenyl-4,5-dihydropyrazole	0.08	16.7	37.5
Pyrazolidine dione	0.21	5.6	4.8
N-Phenylpyrazolidine	0.19	5.6	5.3
Pyrrole	3.1	13.3	0.3
N-(Carboxyphenyl)pyrrole	0.04	5.6	25
1,3-Benzothiazole	1.27	5.6	0.8
Nitrile ---C≡N	10.01	5.6	0.1
Trifluoromethyl CF₃	4.49	5.6	0.2

^{a} Dashed lines represent any bond type, and A represents any atom except hydrogen ^{b} The number of compounds in the active set was 18 (see Table 1 and Figure 2).

inhibitor (compound **1**) had only four clusters (Supporting Information, Figure S1) allowing us to identify a conformation that correlated quite well with the pharmacophore model. Although conformation 2 is stabilized by hydrogen bonds between the carboxyl group and furan (3.2 Å) and carbonyl (2.3 Å) oxygen atoms, it was 2.70 kcal/mol higher in energy than the global minimum conformation 1. We also found that global minimum conformation of compound **1** had the best correspondence to the pharmacophore model of Panchal et al.[14] (Figures 6 and 7). Consequently, conformer 1 can be regarded as a close approximation to the bioactive conformation of compound **1**, and it is reasonable to attribute the benzene ring
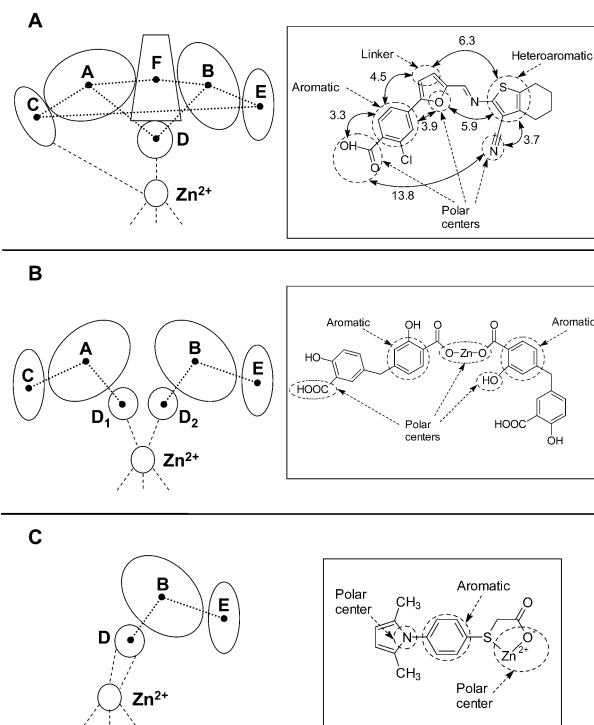

Figure 5. Pharmacophore model of LF inhibitors with hypothetical derivatives. Panel A: Spatial relationships in the published pharmacophore model reported by Panchal et al.[14] Inset: Pharmacophore modeling of compound **9**. Panel B: Hypothetical dimeric pharmacophore model with monodentate Zn²⁺ coordination. Inset: Modeling Zn²⁺ coordination for compound **4**. Panel C: Hypothetical monomeric pharmacophore model with bidentate Zn²⁺ coordination. Inset: Modeling Zn²⁺ coordination for compound **58**. The distances indicated in the insets were calculated for the molecular conformation with the lowest energy (Table 7).

to the aromatic pharmacophore point **B** and to assign the furan oxygen atom to the central polar region **D**. In this case, substituents R¹ in the α-position of the furan ring would overlap with each other in suitable conformations. For compounds **2**, **5**, **7−10**, **12**, **15**, **17**, and **18**, it was possible, from the array of representative conformers, to choose a geometry that provided the best overlap with the putative bioactive conformation of inhibitor **1**. Polar substituents (chlorine atoms, carbonyl and carboxyl groups, and nitrogen atoms (heterocycle of compound **8**)) in this superimposition were close to a point that can be regarded as polar center **C** (Figure 6). We refined the superimposition by including distances from pharmacophore center **C** to the polar groups in the rms fit, for compounds having such groups in the vicinity of **C**. The overlaid geometries thus obtained are shown in Figure 6, and individual compounds in the appropriate conformations are shown in Figure 7 together with the pharmacophoric centers indicated for clarity. It can be seen that the hydrophobic center corresponding to region **A** in this overlay contains aromatic or heteroaromatic rings, and the third polar center **E** is clearly located in the vicinity of electron-acceptor substituents in para and meta positions of the phenyl ring (Figure 6). Finally, neutral linker **F** is placed near the β-carbon atoms of furan moieties in the overlay. Overall, the total arrangement of overlaid molecules corresponds extremely well with the active site of LF, as modeled previously.[14]

    Table 7 contains the distances between pharmacophoric centers obtained by us in comparison with the distances reported by Panchal et al.[14] for their pharmacophore model. All distances, except for **B−D**, matched this model within a 0.2 Å tolerance.

Table 5. Characteristics of the Most Potent Carboxylic *N*-Phenylpyrrole LF Inhibitors Found Among the Analogues from Interchim

| | Compound **56** | Compound **57** | Compound **58** |

| | lethal factor | | | | other proteases IC$_{50}$ (μM) | | | | | | |
compd	IC$_{50}$ (μM) microplate assay	K_i (μM)	K_i' (μM)	mode of inhibition	aminopeptidase M	chymotrypsin	kallikrein	elastase	cathepsin B	MMP-9	highest tested concn (μM)
56 (m.w. 261.3)	2.9	1.6	4.6	mixed	N.I.[a]	N.I.	N.I.	15.5	58.3	N.I.	160
57 (m.w. 249.7)	6.8	5.6	7.6	mixed	N.I.	N.I.	N.I.	160.2	7.3	N.I.	175
58 (m.w. 299.3)	7.6	0.9	10.9	mixed	N.I.	N.I.	60.5	124.9	10.1	N.I.	155

[a] N.I., no inhibition seen at the highest concentrations of compound tested (see the last column of the Table).

Table 6. Number of Representative Conformations Found for LF Inhibitors and Relative Energy Levels (kcal/mol) of the Molecules in the Fitted Conformation[a]

compd no.	1	2	5	7	8	9	10	12	15	17	18
N_{conf}	4	16	2	81	50	16	2	10	3	16	8
ΔE^b	0	0.06	2.33	1.03	2.07	2.64	0.03	3.41	0.56	3.66	2.72

[a] The number of representative conformations within 6 kcal/mol of the global energy minimum are indicated. [b] Energy difference with respect to the global minimum for the lowest energy conformation of each compound.

Good agreement among these values indicates that the geometries used for the superimposition were close to bioactive conformations of the compounds under investigation. Although a 6 kcal/mol energy gap was used during the conformational search, most of these conformations were within 3 kcal/mol above the corresponding global minima (Table 6), a value generally considered as acceptable in pharmacophore mapping studies.[43] It should be noted that polar center **B** coincides with benzene rings in the superimposed molecules, whereas molecular moieties corresponding to center **A** have a more diverse character, comprising aromatic and heteroaromatic cycles as well as acyclic fragments of hydrophobic nature. Although the position of Zn^{2+} with respect to the centers also is not defined in the published pharmacophore model,[14] it is reasonable to associate it with the position of polar region **D** in the middle of the model (Figure 5A). Indeed, the crystal structure of LF in complex with a small-molecule inhibitor shows that its urea moiety, containing polar center **D** and a linker **F**, is very close to the catalytic Zn^{2+}, and the distance between the urea group and Zn^{2+} was determined to be within 4 Å, at a resolution of 2.9 Å.[14] At these distances (<2.05 Å), donor−acceptor coordination interactions between Zn^{2+} and polar groups of a given protease inhibitor would be possible.[44,45]

It should be noted that the superimposed compounds did not always contain groups that could be attributed to all of the pharmacophoric centers shown in Figures 6 and 7. For example, inhibitors **5** and **10** only partially occupied space within the overlaid structures. However, partial binding within the active site could also lead to inhibition of the enzyme. For the remaining 10 compounds of the 21 active inhibitors, it is difficult to suggest a defined pharmacophore model, at least for their conformations found within the 6 kcal/mol energy gap. Nevertheless, it is possible to propose mechanisms in which these and other LF inhibitors could interact with the active site. For example, carboxylic acid groups in compounds **4**, **6**, **11**, **13**, **14**, **16**, and **56−58** as well as sulfamate and sulfonamide groups in compounds **6**, **13**, and **16** could act as donors for the catalytic
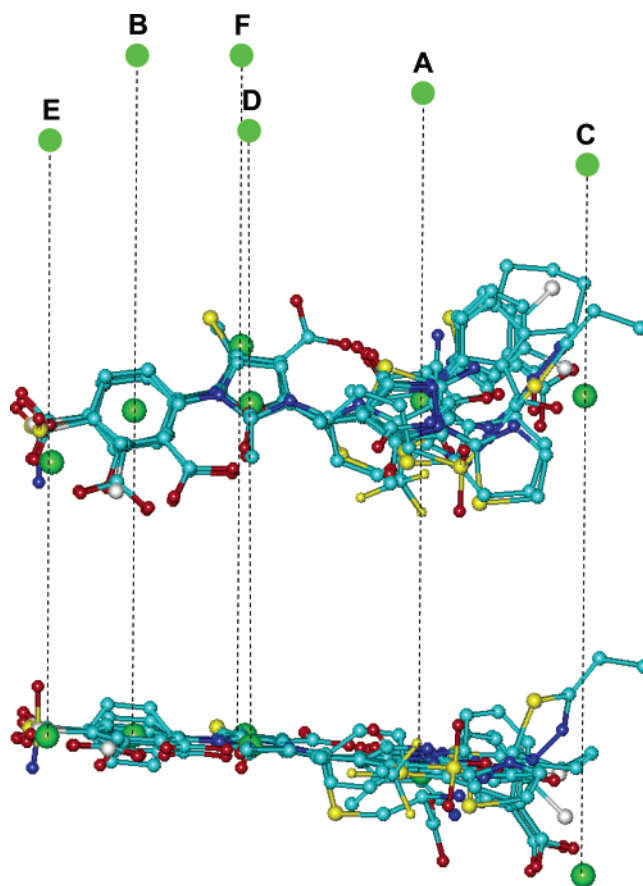
Figure 6. Comparison of LF inhibitor conformation with the that of published LF inhibitor pharmacophore model. A spatial overlay of 11 representative compounds on the published pharmacophore coordinates is shown. Compound conformations shown represent the best rms fit from all clusters within 6 kcal/mol of the global energy minimum. The superimposition is shown in two projections, and the green ellipses are located at the pharmacophore centers of the superimposition in both projections. The centers are also indicated at the top of the Figure for clarity, with letter notation corresponding to the hydrophobic (**A** and **B**), polar (**C**, **D**, and **E**), and linker (**F**) centers, as previously reported.[14] For all structures, carbon is sky-blue, nitrogen is blue, oxygen is red, sulfur and bromine are yellow, and chlorine is white.

Zn^{2+}.[36,46] Likewise, inhibitors **3**, **6**, **11**, and **14** could be ligated to Zn^{2+} through one of the carbonyl oxygen atoms in the linker chain or heterocycle. Analogous to the pharmacophore model, the spatial arrangement of two aromatic and two polar centers in inhibitors **4**, **11**, and **56−58** could result in a symmetrical, dimeric monodentate model (Figure 5B). For example, the inset

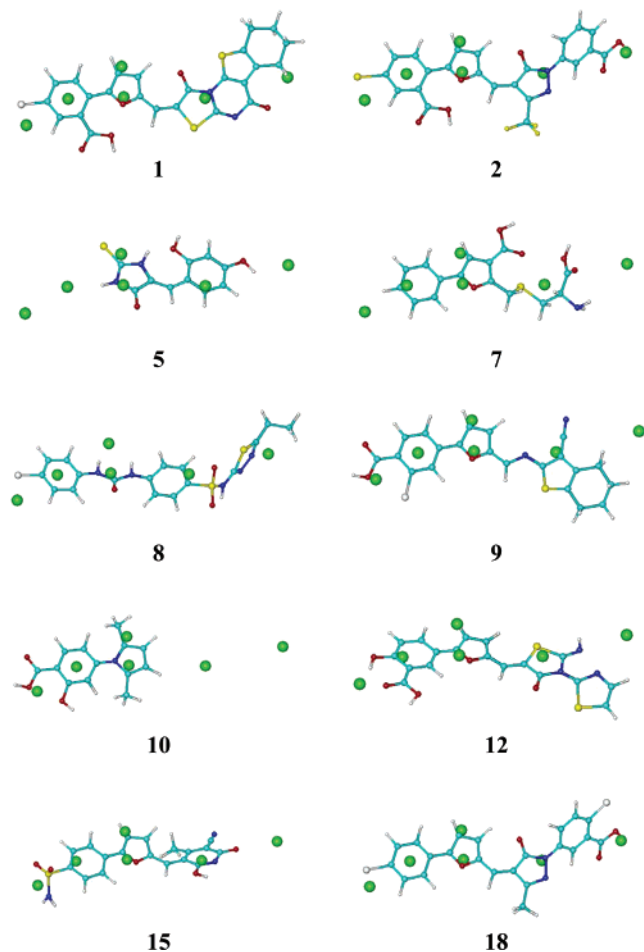**Figure 7.** Superimposition of individual LF inhibitors on the LF pharmacophore model. Model details are as described in the legend for Figure 6.

Table 7. Distances Between Pharmacophore Centers in the Superimposition of Representative Conformations of LF Inhibitors and Comparison with the Published Pharmacophore Model[a]

Pharmacophore Centers	A−C	A−D	A−F	B−F	B−D	B−E
our data	6.4	5.4	5.9	4.1	3.6	3.2
published model[b]	6.5	5.6	5.7	3.9	4.1	3.1

[a] All distances are in Å. [b] Model for comparison was published by Panchal et al.[14] Note: Panchal et al.[14] reported a distance of 17.6 Å between C−E, whereas this distance was 18.7 Å in our model. Distance C−E is highly sensitive to small conformational changes.

of Figure 5B shows a model of compound **4** with this type of Zn^{2+} coordination. In this model, chelation of the compounds with catalytic Zn^{2+} could stabilize hydrophobic interactions. We also considered that chelation of Zn^{2+} by several electron pairs from one inhibitor molecule alone is not likely in the dimeric model because Zn^{2+} is strongly coordinated with three protein side chains (His 686, His 690, and Glu 735) of the enzyme core.[29] Therefore, we suggest that the thiomethylcarboxylic moiety of compound **56** is in a monomeric bidentate conformation, with the sulfur and hydroxyl oxygen atoms directed toward the Zn^{2+} (Figure 5C, inset). Ultimately, crystallographic studies will be required to determine the precise binding mode of these inhibitors in the active site of LF and perform docking studies. Unfortunately, we were not able to perform docking studies or conformational searches with the excluded volumes of the compounds because of the significant flexibility of both enzyme and inhibitor molecules. However, because many of our lead

compounds overlapped the published pharmacophore model, which fit with the crystal structure of the LF binding pocket,[14] it is reasonable to propose that these compounds could also fit into the LF binding groove.

Conclusions

We utilized high-throughput screening of a large chemical diversity library to select unique small-molecule inhibitors of anthrax LF, and identified 21 such compounds. A number of these lead compounds were highly active, with IC_{50} values of ~1−3 μM, making them promising candidates for further evaluation in vitro and eventually in vivo. These compounds inhibited LF activity in microplate- and HPLC-based enzymatic assays and were relatively specific for LF compared to that of a range of other proteases tested. Kinetics of inhibition indicated that all compounds were mixed-mode competitive inhibitors, suggesting that they can bind to the active site region of LF but may not fully compete with the 14-mer peptide substrate. However, further crystallographic analysis of these inhibitors complexed with LF will be needed to provide more definitive information on this issue. Nevertheless, the most potent compounds represent interesting hits for further optimization. Indeed, a number of compounds (**1**, **2**, **5**−**7**, **9-12**, **14**, **15**, **17**, and **18**) have little similarity to previously published competitive inhibitors of LF.[21,22] Most of the inhibitors identified (~62%) were phenylfuran, phenylpyrazole, and phenylpyrrole carboxylic derivatives, suggesting that sizable libraries of these types of derivatives could be screened *in silico* to search for further LF inhibitors. Furthermore, compounds **3** and **8**, containing 1,3-dithian-2-ylidene and *N,N*-diphenylurea-sulfonamide fragments, respectively, represent completely new structural classes of highly active LF inhibitors. Importantly, molecular modeling showed that a selection of these inhibitors fit quite well with the previously published pharmacophore model developed for LF inhibitors.[14] Therefore, our data support the validity of this model and substantiate its value as a tool for virtual screening of chemical databases to detect novel lead structures for LF inhibitors.

Experimental Section

Compounds. The chemical diversity set of 10 000 compounds was obtained from TimTec, Inc. (Newark, DE). This commercial library is comprises a random selection of 10 000 drug-like compounds. Additional compounds were synthesized by Interchim (Montluçon, France).

Library Screening and Kinetic Measurements. We screened the 10 000-compound chemical diversity set for LF inhibitory activity. The compounds were originally dissolved in 100% dimethyl sulfoxide (DMSO) at a concentration of 2 mg/mL, and the final concentration of DMSO in the reaction mix ranged from 0.5 to 2%. An analysis of DMSO as a background control showed no effect on enzyme activity (>95% enzyme activity) at concentrations ≤2% DMSO. HTS was performed in black flat-bottom 96-well microtiter plates, as described by Panchal et al.[14] Briefly, a solution containing 40 mM HEPES at pH 7.2, 0.05% (v/v) Tween 20, 100 μM $CaCl_2$, and up to 5 nM recombinant LF (Calbiochem, San Diego, CA) was added to wells containing 20 μg/mL of each compound. The reaction was initiated by addition of 2 μM fluorogenic LF protease substrate III (Calbiochem) in a final reaction volume of 100 μL/well. Kinetic measurements were obtained every minute for 10 min at 27 °C using a Fluroscan Ascent FL (Thremo Electron, Waltham, MA) with excitation and emission wavelengths at 355 and 460 nm, respectively.

For selected lead compounds, the concentrations of inhibitor that caused 50% inhibition of the enzymatic reaction (IC_{50}) were calculated by plotting percent inhibition against the logarithm of inhibitor concentration (at least 6 points) and are mean values of

at least three experiments with relative standard deviations <15%. K_m and V_{max} were calculated using the double-reciprocal Lineweaver−Burk plot of rate versus substrate concentration, and the values of K_i and K_i' were found using replots of inhibitor concentration against K_m/V_{max} and I/V_{max} values, respectively.[47] Lineweaver−Burk plots were linear ($R^2 = 0.998$) over the relevant concentration range of fluorogenic substrate ($0.5−3$ μM), indicating that the inner filter effect was very small at substrate concentrations ≤ 3 μM and our typical conditions of fluorescence measurement using black flat-bottom 96 well microtiter plates.[48] Kinetic studies consisted of three independent experiments with four replicates in each experiment.

HPLC Assay. Reaction mixtures (20 μL total volume) containing 40 mM HEPES at pH 7.2, 0.05% (v/v) Tween 20, 100 μM CaCl$_2$, and 2 μM fluorogenic LF protease substrate III, with or without inhibitor, were incubated with 0.5 μg/mL of LF for 30 min at 27 °C. The reactions were stopped by adding 180 μL of 70% (v/v) acetonitrile in 0.1% (v/v) trifluoroacetic acid (TFA), and the products were separated by reverse-phase HPLC on an automated HPLC system (Shimadzu, Torrance, CA) with a Phenomenex Jupiter C18 300A column (5 μm, 25 × 0.46 cm) eluted with acetonitrile/water (35/65, v/v) containing 0.1% (v/v) TFA at a flow rate of 0.8 mL/min at 30 °C over 15 min. The elution of LF inhibitors was monitored using a diode array detector (Shimadzu SPD-M10A VP) at specific wavelength regions where the inhibitor showed greatest absorbance. The fluorescence peak of the *C*-terminal cleavage product was detected using a fluorescence detector (Shimadzu RF-10A XL) at excitation and emission wavelengths of 340 and 430 nm, respectively. For the selected inhibitors, the IC$_{50}$ values were evaluated using six different concentrations of the inhibitor ranging from 0.3 to 40 μg/mL and measuring the fluorescence peak of the *C*-terminal cleavage product.

The incubation of the fluorogenic substrate with LF resulted in one new peak in the chromatogram ($R_t = 5.84$), with a concomitant decrease in peak height of the substrate peak ($R_t = 4.08$) (Figure 3), and the rate of increase in the peak fluorescence was linearly related to the amount of LF (Figure 3, inset). A comparative analysis of microplate- and HPLC-based assays resulted in a linear correlation between the values of fluorescence signals ($R^2 > 0.999$), measured at same time point of incubation of the substrate with LF. In addition, the peaks of selected inhibitors and the fluorescence *C*-terminal cleavage product were completely separated at the indicated elution conditions.

Analysis of Inhibitor Specificity. Selected compounds were evaluated for their ability to inhibit a range of proteases in 100 μL reaction volumes at 30 °C. Aminopeptidase M inhibitory activity was determined by a modification of the method of Ishida et al.[49] Reaction mixtures contained 0.1 M Tris-HCl buffer at pH 7.0, 0.05% (v/v) Tween 20, 2 mU porcine kidney aminopeptidase M (Calbiochem), test compounds, and 0.4 mM L-alanyl-*p*-nitroanilide (Calbiochem). Pro-MMP-9 was activated at 37 °C for 2 h in buffer A (50 mM Tris-HCl at pH 7.6, 150 mM NaCl, 5 mM CaCl$_2$, 0.01% Brij 35) with 0.2 mM *p*-aminophenylmercuric acetate. The MMP-9 inhibition assay was performed in reaction mixtures containing buffer A, 3 nM MMP-9 (Calbiochem), test compounds, and 20 μM MMP substrate III (DABCYL-GABA-Pro-Gln-Gly-Leu-Glu-(EDANS)-Ala-Lys-NH$_2$, Calbiochem). The kallikrein inhibition assay was performed in reaction mixtures containing 50 mM Tris-HCl at pH 8.0, 100 mM NaCl, 0.05% (v/v) Tween-20, 2 nM human plasma kallikrein (Calbiochem), test compounds, and 50 μM substrate (benzyloxycarbonyl-Phe-Arg-7-amino-4-methylcoumarin, Calbiochem). The elastase inhibition assay was performed in reaction mixtures containing 200 mM Tris-HCl at pH 7.5, 0.001% HSA, 20 mU/mL of human neutrophil elastase (Calbiochem), test compounds, and 750 μM elastase substrate (MeOSuc-Ala-Ala-Pro-Val-7-amino-4-methylcoumarin, Calbiochem). The chymotrypsin inhibition assay was performed in reaction mixtures containing 50 mM Tris-HCl at pH 8.0, 30 nM human pancreas chymotrypsin (Calbiochem), test compounds, and 250 μM chymotrypsin substrate (Suc-Ala-Ala-Pro-Phe-7-amino-4-methylcoumarin, Calbiochem). The cathepsin B inhibition assay was performed in reaction mixtures containing 250 mM sodium potassium phosphate buffer at pH 6.0, 150 nM human liver cathepsin B (Calbiochem), test compounds, and 400 μM cathepsin B substrate III (benzyloxycarbonyl-Arg-Arg-7-amino-4-methylcoumarin, Calbiochem). Reactions for aminopeptidase M were monitored at 405 nm using a SpectraMax Plus microtiter plate reader (Molecular Devices, Sunnyvale, CA). For all other proteases, fluorescence substrate cleavage was monitored with a Fluoroskan Ascent FL microtiter plate reader with excitation and emission wavelengths of 355 and 460 nm, respectively.

Conformational Analysis. For 11 inhibitors, sets of conformations were generated using the Conformational Search Module, as implemented in HyperChem Version 7.0 (Hypercube, Inc., Canada). The systematic search of conformations for each compound was performed by energy minimization, starting with 1000 initial geometries at random values of torsion angles about exocyclic single bonds and chemical bonds within nonaromatic cycles. Energy was minimized by the Polak-Ribiere conjugate gradient method with the MM+ force field (HyperChem). Attainment of an rms gradient <0.02 kcal/mol·Å was used as the termination condition for minimization. Conformations were compared and considered as equal if their rms difference in atomic coordinates was less than 0.25 Å, and unique conformations were clustered as described.[42] Independent conformations obtained after cluster analysis were then optimized by semiempirical parametric method 3 (PM3) and used for alignment and generation of the pharmacophore.

To determine a geometry favorable for the interaction of an inhibitor with the enzyme site, we fitted conformations of compound **1** to the pharmacophore model developed previously by Panchal et al.[14] for a different set of LF inhibitors. The conformation chosen (see Results) was then used as a template for alignment of representative conformations of the other selected compounds. Using the resulting overlay of structures, the coordinates of pharmacophore centers were determined from the positions of benzene rings (**B**), polar substituents in para and ortho positions (**E**), electron-withdrawing atoms in the five-membered ring linked to benzene (**D**), and aromatic or heteroaromatic substructures near this ring (**A**). Center **C** was located in the vicinity of polar groups present in some compounds far from the five-membered ring. The overlay of structures was refined by a rms fitting of the conformations to the pharmacophore points.

Supporting Information Available: Structures and activities of the carboxylic and *N*-sulfonylated phenylfuran derivatives, carboxylic and sulfonamide derivatives of 1-phenyl-4,5-dihydro-5-pyrazolone, and carboxylic *N*-penylpyrrole derivatives as well as an example of the optimization of LF inhibitor conformation. This material is available free of charge via the Internet at http://pubs.acs.org.

References

(1) Keim, P.; Smith, K. L. Bacillus anthracis evolution and epidemiology. *Curr. Top. Microbiol. Immunol.* **2002**, *271*, 21−32.

(2) Baillie, L. W. Bacillus anthracis, a story of nature subverted by man. *Lett. Appl. Microbiol.* **2005**, *41*, 227−229.

(3) Collier, R. J.; Young, J. A. Anthrax toxin. *Annu. Rev. Cell Dev. Biol.* **2003**, *19*, 45−70.

(4) Abrami, L.; Reig, N.; van der Goot, F. G. Anthrax toxin: the long and winding road that leads to the kill. *Trends Microbiol.* **2005**, *13*, 72−78.

(5) Krantz, B. A.; Melnyk, R. A.; Zhang, S.; Juris, S. J.; Lacy, D. B.; Wu, Z.; Finkelstein, A.; Collier, R. J. A phenylalanine clamp catalyzes protein translocation through the anthrax toxin pore. *Science* **2005**, *309*, 777−781.

(6) Mock, M.; Mignot, T. Anthrax toxins and the host: a story of intimacy. *Cell. Microbiol.* **2003**, *5*, 15−23.

(7) Dixon, T. C.; Meselson, M.; Guillemin, J.; Hanna, P. C. Anthrax. *N. Engl. J. Med.* **1999**, *341*, 815−826.

(8) Komiyama, T.; Swanson, J. A.; Fuller, R. S. Protection from anthrax toxin-mediated killing of macrophages by the combined effects of furin inhibitors and chloroquine. *Antimicrob. Agents Chemother.* **2005**, *49*, 3875−3882.

(9) Huber, M.; Vor Dem, E. U.; Grunow, R.; Bessler, W. G. Generation of mouse polyclonal and human monoclonal antibodies against *Bacillus anthracis* toxin. *Drugs Exp. Clin. Res.* **2005**, *31*, 35−43.

(10) Mourez, M.; Kane, R. S.; Mogridge, J.; Metallo, S.; Deschatelets, P.; Sellman, B. R.; Whitesides, G. M.; Collier, R. J. Designing a polyvalent inhibitor of anthrax toxin. *Nat. Biotechnol.* **2001**, *19*, 958−961.

(11) Tonello, F.; Seveso, M.; Marin, O.; Mock, M.; Montecucco, C. Screening inhibitors of anthrax lethal factor. *Nature* **2002**, *418*, 386.

(12) Montecucco, C.; Tonello, F.; Zanotti, G. Stop the killer: how to inhibit the anthrax lethal factor metalloprotease. *Trends Biochem. Sci.* **2004**, *29*, 282−285.

(13) Kim, C.; Gajendran, N.; Mittrucker, H. W.; Weiwad, M.; Song, Y. H.; Hurwitz, R.; Wilmanns, M.; Fischer, G.; Kaufmann, S. H. Human α-defensins neutralize anthrax lethal toxin and protect against its fatal consequences. *Proc. Natl. Acad. Sci. U.S.A.* **2005**, *102*, 4830−4835.

(14) Panchal, R. G.; Hermone, A. R.; Nguyen, T. L.; Wong, T. Y.; Schwarzenbacher, R.; Schmidt, J.; Lane, D.; McGrath, C.; Turk, B. E.; Burnett, J.; Aman, M. J.; Little, S.; Sausville, E. A.; Zaharevitz, D. W.; Cantley, L. C.; Liddington, R. C.; Gussio, R.; Bavari, S. Identification of small molecule inhibitors of anthrax lethal factor. *Nat. Struct. Mol. Biol.* **2004**, *11*, 67−72.

(15) Turk, B. E.; Wong, T. Y.; Schwarzenbacher, R.; Jarrell, E. T.; Leppla, S. H.; Collier, R. J.; Liddington, R. C.; Cantley, L. C. The structural basis for substrate and inhibitor selectivity of the anthrax lethal factor. *Nat. Struct. Mol. Biol.* **2004**, *11*, 60−66.

(16) Min, D. H.; Tang, W. J.; Mrksich, M. Chemical screening by mass spectrometry to identify inhibitors of anthrax lethal factor. *Nat. Biotechnol.* **2004**, *22*, 717−723.

(17) Lee, L. V.; Bower, K. E.; Liang, F. S.; Shi, J.; Wu, D.; Sucheck, S. J.; Vogt, P. K.; Wong, C. H. Inhibition of the proteolytic activity of anthrax lethal factor by aminoglycosides. *J. Am. Chem. Soc.* **2004**, *126*, 4774−4775.

(18) Numa, M. M.; Lee, L. V.; Hsu, C. C.; Bower, K. E.; Wong, C. H. Identification of novel anthrax lethal factor inhibitors generated by combinatorial Pictet−Spengler reaction followed by screening in situ. *ChemBioChem* **2005**, *6*, 1002−1006.

(19) Fridman, M.; Belakhov, V.; Lee, L. V.; Liang, F. S.; Wong, C. H.; Baasov, T. Dual effect of synthetic aminoglycosides: antibacterial activity against *Bacillus anthracis* and inhibition of anthrax lethal factor. *Angew. Chem., Int. Ed.* **2005**, *44*, 447−452.

(20) Kocer, S. S.; Walker, S. G.; Zerler, B.; Golub, L. M.; Simon, S. R. Metalloproteinase inhibitors, nonantimicrobial chemically modified tetracyclines, and ilomastat block *Bacillus anthracis* lethal factor activity in viable cells. *Infect. Immun.* **2005**, *73*, 7548−7557.

(21) Forino, M.; Johnson, S.; Wong, T. Y.; Rozanov, D. V.; Savinov, A. Y.; Li, W.; Fattorusso, R.; Becattini, B.; Orry, A. J.; Jung, D.; Abagyan, R. A.; Smith, J. W.; Alibek, K.; Liddington, R. C.; Strongin, A. Y.; Pellecchia, M. Efficient synthetic inhibitors of anthrax lethal factor. *Proc. Natl. Acad. Sci. U.S.A.* **2005**, *102*, 9499−9504.

(22) Johnson, S. L.; Jung, D.; Forino, M.; Chen, Y.; Satterthwait, A.; Rozanov, D. V.; Strongin, A. Y.; Pellecchia, M. Anthrax lethal factor protease inhibitors: synthesis, SAR, and structure-based 3D QSAR studies. *J. Med. Chem.* **2006**, *49*, 27−30.

(23) Xiong, Y.; Wiltsie, J.; Woods, A.; Guo, J.; Pivnichny, J. V.; Tang, W.; Bansal, A.; Cummings, R. T.; Cunningham, B. R.; Friedlander, A. M.; Douglas, C. M.; Salowe, S. P.; Zaller, D. M.; Scolnick, E. M.; Schmatz, D. M.; Bartizal, K.; Hermes, J. D.; MacCoss, M.; Chapman, K. T. The discovery of a potent and selective lethal factor inhibitor for adjunct therapy of anthrax infection. *Bioorg. Med. Chem. Lett.* **2006**, *16*, 964−968.

(24) Jiao, G. S.; Cregar, L.; Goldman, M. E.; Millis, S. Z.; Tang, C. Guanidinylated 2,5-dideoxystreptamine derivatives as anthrax lethal factor inhibitors. *Bioorg. Med. Chem. Lett.* **2006**, *16*, 1527−1531.

(25) Dell'Aica, I.; Dona, M.; Tonello, F.; Piris, A.; Mock, M.; Montecucco, C.; Garbisa, S. Potent inhibitors of anthrax lethal factor from green tea. *EMBO Rep.* **2004**, *5*, 418−422.

(26) McGovern, S. L.; Caselli, E.; Grigorieff, N.; Shoichet, B. K. A common mechanism underlying promiscuous inhibitors from virtual and high-throughput screening. *J. Med. Chem.* **2002**, *45*, 1712−1722.

(27) Blanchard, J. E.; Elowe, N. H.; Huitema, C.; Fortin, P. D.; Cechetto, J. D.; Eltis, L. D.; Brown, E. D. High-throughput screening identifies inhibitors of the SARS coronavirus main proteinase. *Chem. Biol.* **2004**, *11*, 1445−1453.

(28) Cornish-Bowden, A. *Fundamentals of Enzyme Kinetics*; Butterworth & Company, Ltd.: Woburn, MA, 1979.

(29) Pannifer, A. D.; Wong, T. Y.; Schwarzenbacher, R.; Renatus, M.; Petosa, C.; Bienkowska, J.; Lacy, D. B.; Collier, R. J.; Park, S.; Leppla, S. H.; Hanna, P.; Liddington, R. C. Crystal structure of the anthrax lethal factor. *Nature* **2001**, *414*, 229−233.

(30) Tonello, F.; Naletto, L.; Romanello, V.; Dal, M. F.; Montecucco, C. Tyrosine-728 and glutamic acid-735 are essential for the metallo-proteolytic activity of the lethal factor of *Bacillus anthracis*. *Biochem. Biophys. Res. Commun.* **2004**, *313*, 496−502.

(31) Krantz, A. A classification of enzyme−inhibitors. *Bioorg. Med. Chem. Lett.* **1992**, *2*, 1327−1334.

(32) Thompson, S. A.; Andrews, P. R.; Hanzlik, R. P. Carboxyl-modified amino acids and peptides as protease inhibitors. *J. Med. Chem.* **1986**, *29*, 104−111.

(33) Babine, R. E.; Bender, S. L. Molecular recognition of protein−ligand complexes: Applications to drug design. *Chem. Rev.* **1997**, *97*, 1359−1472.

(34) Pruitt, J. R.; Pinto, D. J.; Galemmo, R. A., Jr.; Alexander, R. S.; Rossi, K. A.; Wells, B. L.; Drummond, S.; Bostrom, L. L.; Burdick, D.; Bruckner, R.; Chen, H.; Smallwood, A.; Wong, P. C.; Wright, M. R.; Bai, S.; Luettgen, J. M.; Knabb, R. M.; Lam, P. Y.; Wexler, R. R. Discovery of 1-(2-aminomethylphenyl)-3-trifluoromethyl-N-[3-fluoro-2′-(aminosulfonyl)[1,1′-biphenyl)]-4-yl]-1H-pyrazole-5-carboxyamide (DPC602), a potent, selective, and orally bio-available factor Xa inhibitor (1). *J. Med. Chem.* **2003**, *46*, 5298−5315.

(35) Kevin, N. J.; Duffy, J. L.; Kirk, B. A.; Chapman, K. T.; Schleif, W. A.; Olsen, D. B.; Stahlhut, M.; Rutkowski, C. A.; Kuo, L. C.; Jin, L.; Lin, J. H.; Emini, E. A.; Tata, J. R. Novel HIV-1 protease inhibitors active against multiple PI-resistant viral strains: coadministration with indinavir. *Bioorg. Med. Chem. Lett.* **2003**, *13*, 4027−4030.

(36) Huang, Q. Q.; Huang, M.; Nan, F. J.; Ye, Q. Z. Metalloform-selective inhibition: synthesis and structure−activity analysis of Mn(II)-form-selective inhibitors of *Escherichia coli* methionine aminopeptidase. *Bioorg. Med. Chem. Lett.* **2005**, *15*, 5386-5391.

(37) Lu, Z.; Bohn, J.; Rano, T.; Rutkowski, C. A.; Simcoe, A. L.; Olsen, D. B.; Schleif, W. A.; Carella, A.; Gabryelski, L.; Jin, L.; Lin, J. H.; Emini, E.; Chapman, K.; Tata, J. R. Orally bioavailable highly potent HIV protease inhibitors against PI-resistant virus. *Bioorg. Med. Chem. Lett.* **2005**, *15*, 5311−5314.

(38) Bellu, S.; Hure, E.; Trape, M.; Rizzotto, M.; Sutich, E.; Sigrist, M.; Moreno, V. The interaction between mercury(II) and sulfathiazole. *Quim. Nova* **2003**, *26*, 188−192.

(39) Yoshihara, T.; Druzhinin, S. I.; Zachariasse, K. A. Fast intramolecular charge transfer with a planar rigidized electron donor/acceptor molecule. *J. Am. Chem. Soc.* **2004**, *126*, 8535−8539.

(40) Lepailleur, A.; Bureau, R.; Paillet-Loilier, M.; Fabis, F.; Saettel, N.; Lemaitre, S.; Dauphin, F.; Lesnard, A.; Lancelot, J. C.; Rault, S. Molecular modeling studies focused on 5-HT7 versus 5-HT1A selectivity. Discovery of novel phenylpyrrole derivatives with high affinity for 5-HT7 receptors. *J. Chem. Inf. Model.* **2005**, *45*, 1075−1081.

(41) Nicklaus, M. C.; Wang, S. M.; Driscoll, J. S.; Milne, G. W. A. Conformational-changes of small molecules binding to proteins. *Bioorg. Med. Chem.* **1995**, *3*, 411−428.

(42) Shenkin, P. S.; Mcdonald, D. Q. Cluster-analysis of molecular-conformations. *J. Comput. Chem.* **1994**, *15*, 899−916.

(43) Wermuth, C. G.; Langer, T. Pharmacophore Identification. In *3D QSAR in Drug Design. Theory Methods and Applications*; Kubinyi, H., Ed.; ESCOM: Leiden, The Netherlands, 1993; pp 117−136.

(44) Brandstetter, H.; Grams, F.; Glitz, D.; Lang, A.; Huber, R.; Bode, W.; Krell, H. W.; Engh, R. A. The 1.8-A crystal structure of a matrix metalloproteinase 8-barbiturate inhibitor complex reveals a previously unobserved mechanism for collagenase substrate recognition. *J. Biol. Chem.* **2001**, *276*, 17405−17412.

(45) Voisin, S.; Rognan, D.; Gros, C.; Ouimet, T. A three-dimensional model of the neprilysin 2 active site based on the X-ray structure of neprilysin. Identification of residues involved in substrate hydrolysis and inhibitor binding of neprilysin 2. *J. Biol. Chem.* **2004**, *279*, 46172−46181.

(46) Nishino, N.; Powers, J. C. Design of potent reversible inhibitors for thermolysin. Peptides containing zinc coordinating ligands and their use in affinity chromatography. *Biochemistry* **1979**, *18*, 4340−4347.

(47) O'Donohue, M. J.; Beaumont, A. The roles of the prosequence of thermolysin in enzyme inhibition and folding in vitro. *J. Biol. Chem.* **1996**, *271*, 26477−26481.

(48) Liu, Y.; Kati, W.; Chen, C. M.; Tripathi, R.; Molla, A.; Kohlbrenner, W. Use of a fluorescence plate reader for measuring kinetic parameters with inner filter effect correction. *Anal. Biochem.* **1999**, *267*, 331−335.

(49) Ishida, K.; Kato, T.; Murakami, M.; Watanabe, M.; Watanabe, M. F. Microginins, zinc metalloproteases inhibitors from the cyanobacterium *Microcystis aeruginosa*. *Tetrahedron* **2000**, *56*, 8643−8656.